BIOCHEMISTRY
including biophysical chemistry & molecular biology

Article

pubs.acs.org/biochemistry

Overexpression in Yeast, Photocycle, and *in Vitro* Structural Change of an Avian Putative Magnetoreceptor Cryptochrome4

Hiromasa Mitsui, Toshinori Maeda, Chiaki Yamaguchi, Yusuke Tsuji, Ryuji Watari, Yoko Kubo, Keiko Okano, and Toshiyuki Okano*

Department of Electrical Engineering and Bioscience, Graduate School of Advanced Science and Engineering, Waseda University, Wakamatsu-cho 2-2, Shinjuku-ku, Tokyo 162-8480, Japan

ABSTRACT: Cryptochromes (CRYs) have been found in a wide variety of living organisms and can function as blue light photoreceptors, circadian clock molecules, or magnetoreceptors. Non-mammalian vertebrates have CRY4 in addition to the CRY1 and CRY2 circadian clock components. Though the function of CRY4 is not well understood, chicken CRY4 (cCRY4) may be a magnetoreceptor because of its high level of expression in the retina and light-dependent structural changes in retinal homogenates. To further characterize the photosensitive nature of cCRY4, we developed an expression system using budding yeast and purified cCRY4 at yields of submilligrams of protein per liter with binding of the flavin adenine dinucleotide (FAD) chromophore. Recombinant cCRY4 dissociated from anti-cCRY4 C1 mAb, which recognizes the C-terminal region of cCRY4, in a light-dependent manner and showed a light-dependent change in its trypsin digestion pattern, suggesting that cCRY4 changes its conformation with light irradiation in the absence of other retinal factors. Combinatorial analyses with UV−visible spectroscopy and immunoprecipitation revealed that there is chromophore reduction in the cCRY4 photocycle and formation of a flavosemiquinone radical intermediate that is likely accompanied by a conformational change in the carboxyl-terminal region. Thus, cCRY4 seems to be an intrinsically photosensitive and photoswitchable molecule and may exemplify a vertebrate model of cryptochrome with possible function as a photosensor and/or magnetoreceptor.

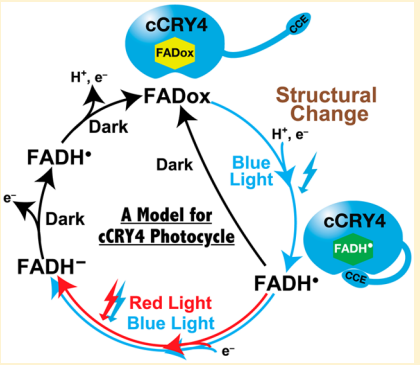

CRY and photolyase [photorepair enzyme (PL)] are flavoproteins that are widely distributed in living organisms such as bacteria, fungi, plants, and animals.[1] Almost all of the CRY/PL family proteins function as photoreceptors for a variety of light-dependent physiological responses such as DNA repair,[2] photomorphogenesis,[3,4] circadian clock function,[5,6] and magnetoreception.[7] Similar to that of PL, the CRY photoreaction may be composed of four steps: (i) photoexcitation of chromophore, flavin adenine dinucleotide (FAD), (ii) intramolecular electron and/or proton transfer, (iii) the conformational change in the protein, and (iv) signal transduction and functional expression. Photoreaction mechanisms of plant CRY and insect type1 CRY have been studied *in vitro* and *in vivo*,[8−17] yet the light-dependent redox cycling of vertebrate cryptochromes remains elusive.

Vertebrates have several classes of CRYs, among which CRY1 and CRY2 function as negative components of the circadian oscillator.[18,19] CRY4 has been found in non-mammalian vertebrates, but it lacks the circadian transcriptional regulatory function[20−22] or the photorepair activity.[20] Although the molecular function(s) of CRY4 proteins is unknown, a photoreceptor and/or light-driven magnetoreceptor function has been suggested on the basis of the following evidence. (i) CRY4 proteins retain carboxyl-terminal extension sequences called CCE regions (cryptochrome carboxyl-terminal extension region), which are not found in cyclobutane pyrimidine dimer PLs and are commonly found in CRYs.[23] (ii) Chicken CRY4 (cCRY4) is strongly expressed in the retina,[24] a postulated central site for magnetoreception.[25] (iii) cCRY4 in chicken retinal homogenates is immunoprecipitated with a higher efficiency in the dark than light by C1 mAb, which recognizes stretches of 14 amino acids (QLTRDDADDPMEMK) within the CCE region.[24] While these results, as well as a change in the molecular structure of the homogenate, are consistent with the idea of cCRY4 photoreception and/or magnetoreception, whether the light-dependent structural change of cCRY4 requires other factors that are endogenously expressed in the chicken retina remains unclear. Although there has been only one preliminary study of photoreaction of cCRY4 expressed in insect cells,[26] the photoreaction mechanism of cCRY4 is still elusive.

To address these unknowns and further examine the molecular nature of cCRY4, we developed an expression system of tagged and nontagged cCRY4 in budding yeast. Spectroscopic and biochemical analyses of recombinant cCRY4 revealed that structural changes with light irradiation occurred through formation of a neutral semiquinone radical form. We also estimated quantum efficiencies of photoreductions occurred in the photocycle.

Received: November 21, 2014
Revised: February 17, 2015
Published: February 17, 2015

DOI: 10.1021/bi501441u
Biochemistry 2015, 54, 1908−1917

MATERIALS AND METHODS

Protein Expression System in the Budding Yeast MaV203. For expression of the GST-cCRY4 protein in budding yeast, we cloned a cDNA encoding GST-cCRY4 into the pYES-DEST52 vector (Life technologies) to generate the expression vector pYES-DEST52-*Gst-cCry4*. The budding yeast MaV203 (ΔGAL4, ΔGAL80) was cotransformed with pYES-DEST52-*Gst-cCry4*, pPC97-Fos (Life technologies), and pPC86-Jun (Life technologies), because MaV203 lacks endogenous GAL4 expression. In this system, DBD-c-Fos, which is a fusion of the GAL4 DNA-binding domain (DBD) and rat c-Fos, and AD-c-Jun, which is a fusion of the GAL4 activation domain (AD) and mouse c-Jun, expressed under the control of a constitutive promoter (P_{ADH1}) bind to the GAL1 promoter (P_{GAL1}) to drive *Gst-cCry4* transcription.

For expression of nontagged cCRY4 protein in MaV203, we cloned *cCry4* cDNA into pYES3/CT (Invitrogen) to generate pYES3-*cCry4*. MaV203 was cotransformed with the pYES3-*cCry4* plasmid and pCL1.[27] In this system, GAL4 protein expressed under the control of a constitutive promoter (P_{ADH1}) transactivates the GAL1 promoter (P_{GAL1}) that drives *cCry4* transcription.

Protein Expression and Purification. MaV203 constitutively expressing GST-cCRY4 or nontagged cCRY4 was cultured with SD medium, -leu, -trp, and -ura for 2 days at 30 °C. The microbial broth was transferred to YPD medium (final yeast density of 6.0−8.0 × 10^6 cells/mL) and cultured at 30 °C in a darkroom. Cultured fluid was centrifuged, and cells were pelleted. Cells were suspended with breaking buffer for GST-cCRY4 [100 mM Tris-HCl (pH 7.5), 100 mM NaCl, 2 mM EDTA, 0.5 mg/L aprotinin, 0.1 mg/L pepstatin, 1.0 mg/L leupeptin, 2 mM PMSF, 5% (v/v) Triton X-100, 5% (v/v) Tween 20, and 5% (v/v) NP-40] or breaking buffer for nontagged cCRY4 [100 mM Tris-HCl (pH 7.5), 100 mM NaCl, 2 mM EDTA, 0.5 mg/L aprotinin, 0.1 mg/L pepstatin, 1.0 mg/L leupeptin, 2 mM PMSF, and 0.2% (v/v) Triton X-100] and then sonicated using the VP-30S UltraS HOMOGENIZER (TAITEC) (duty cycle of 40%, pulse range of 10). The homogenate was centrifuged at 13000*g* for 47 min at 4 °C and cleared. Purification of GST-cCRY4 was performed by using Glutathione Sepharose 4B (GE Healthcare) according to the manufacturer's protocol. Purified GST-cCRY4 was dialyzed against buffer containing 4.17 mM Tris-HCl (pH 7.5) and 8.33 mM NaCl. The dialyzed GST-cCRY4 sample was concentrated to 14-fold using a centrifugal evaporator (EYELA). We obtained a final purified GST-cCRY4 sample that was dissolved into buffer containing 50 mM Tris-HCl (pH 7.5) and 100 mM NaCl. Purification of nontagged cCRY4 was performed by immunoaffinity chromatography using an anti-cCRY4 monoclonal antibody produced as previously reported.[24] The purified nontagged cCRY4 [in buffer containing 50 mM Tris-HCl (pH 7.5), 100 mM NaCl, and 50% (v/v) glycerol] was concentrated by ultrafiltration using the Amicon Ultra-15 30K Centrifugal Filter Device (Millipore).

UV−Visible Spectroscopy. UV−visible absorption spectra were recorded with a UV-2450 spectrophotometer (Shimadzu). The sample in the quartz cell (light path of 1 cm) was kept at a constant temperature in circulating temperature-controlled water in a customized cell holder in which N_2 gas could be applied to the cell to eliminate scattering (Shimadzu). The sample was irradiated with light using an LED (471 nm[28]), power LEDs, royal blue [Philips, Luxeon K2, LXK2-PR14-R00 (λ_{max} = 448−450 nm; $\lambda_{50\%}$ = 429 nm, 467−471 nm; $\lambda_{1\%}$ = 411−413 nm, 495−514 nm)], or blue [OptoSupply OSTCXBC1C1S (λ_{max} = 453 nm; $\lambda_{50\%}$ = 433 nm, 473 nm; $\lambda_{1\%}$ = 403 nm, 518 nm), Luxeon K2, LXK2-PB14-P00 (λ_{max} = 461 nm; $\lambda_{50\%}$ = 441 nm, 481 nm; $\lambda_{1\%}$ = 397 nm, 534 nm)], red [Luxeon K2, LXK2-PD12-R00 (λ_{max} = 628 nm; $\lambda_{50\%}$ = 612 nm, 644 nm; $\lambda_{1\%}$ = 581 nm, 664 nm)], or white [OptoSupply OSW4XME3C1S (λ_{peak} = 458 nm, 557 nm)]. Samples were prepared to contain 50 mM Tris-HCl (pH 7.5), 100 mM NaCl, and 50% (v/v) glycerol and incubated overnight in the dark at 4 °C for complete oxidation of the chromophore FAD. DTT was added as a reducing agent at a final concentration of 5 mM just before the spectroscopic analysis. New samples were used for each experiment.

High-Performance Liquid Chromatography (HPLC) Analysis of the cCRY4 Chromophore. A sample containing purified GST-cCRY4 was dialyzed with 20 mM ammonium bicarbonate, denatured for 3 min at 97 °C, and centrifuged at 20000*g* for 30 min at 4 °C to obtain a supernatant with possible soluble cofactors binding to GST-cCRY4. The supernatant was analyzed via HPLC using the Alliance HPLC system (Waters) and Symmetry300 C18 reversed phase column (Waters) connected to a 5C18-MS-II guard column (COSMOSIL). Samples were eluted using the concentration gradient of acetonitrile (with 0.05% trifluoroacetic acid) in a potassium phosphate buffer [50 mM KH_2PO_4/K_2HPO_4 (pH 5.9) and 0.05% trifluoroacetic acid]. The flow rate was 1 mL/min. Temperatures of the column and the sample were set at 37 and 4 °C, respectively. The fluorescence at 530 nm with excitation at 445 nm was recorded using a 2475 multi lambda fluorescence detector (Waters). Absorbances of 200−800 nm were also recorded using a 2996 PDA detector (Waters).

Immunoprecipitation. Immunoprecipitation of GST-cCRY4 or retinal cCRY4 by C1 mAb was performed as described previously.[24]

Partial Proteolysis with Trypsin. The purified GST-cCRY4 sample was covered with aluminum foil and incubated at 4 °C for 12 h for dark adaptation, followed by addition of DTT at a final concentration of 5 mM. Then, the sequencing grade modified trypsin (Promega) was added to the sample at a trypsin/GST-cCRY4 ratio of 1/800 (w/w, 2.5 ng/2 μg) under dim red light. Trypsin digestion was performed at 25 °C for 30 min under light [F6T5BLB (SANKYO DENKI, λ_{max} = 349 nm; $\lambda_{50\%}$ = 307 nm, 391 nm; $\lambda_{1\%}$ = 259 nm, 420 nm), 1 mW/cm^2] or dark (covered with aluminum foil) conditions. Simultaneously, a no-trypsin control was incubated at 25 °C for 30 min under light conditions. The reaction was halted by adding a quarter of the total volume of 5× sodium dodecyl sulfate−polyacrylamide gel electrophoresis (SDS−PAGE) sample buffer [30% glycerol, 50 mM Tris-HCl (pH 6.8), 10% (w/v) SDS, 250 mM DTT, 10 mM EDTA, and 0.1% CBB R-250], and fragments were analyzed by immunoblotting as described previously.[24]

RESULTS

Expression of Recombinant cCRY4 in Budding Yeast. To perform molecular analysis, we developed expression systems for GST-tagged and nontagged cCRY4 using budding yeast and purified the recombinant cCRY4 proteins. The MaV203 strain was chosen because the cells of this yeast strain could easily be lysed by sonication. GST-cCRY4 and cCRY4 protein expression in yeast was approximately 10 mg in a 5 L culture, and we obtained after purification 354 μg of GST-

DOI: 10.1021/bi501441u
Biochemistry 2015, 54, 1908−1917

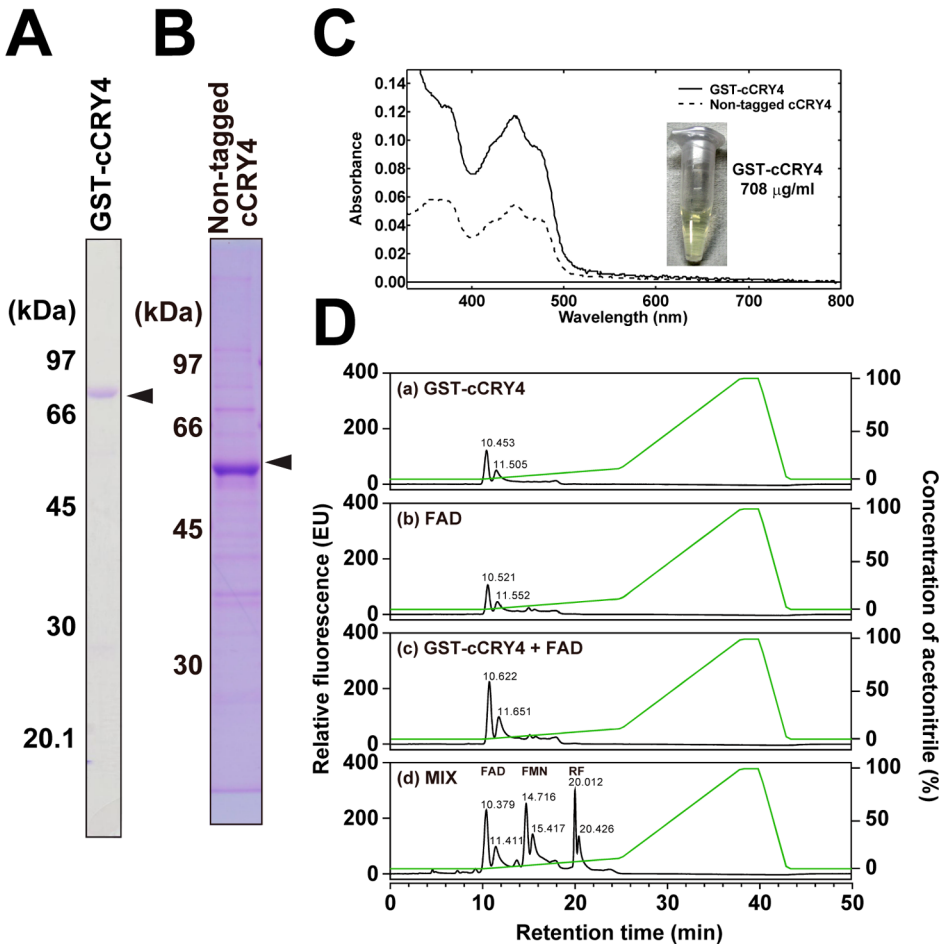

Figure 1. Expression in yeast, purification, and chromophore characterization of recombinant cCRY4. SDS−PAGE analysis and CBB staining of purified (A) GST-cCRY4 (calculated molecular mass of 88094 Da) and (B) nontagged cCRY4 (calculated molecular mass of 61063 Da). (C) UV−visible absorption spectra of GST-cCRY4 (—) and nontagged cCRY4 (---). The inset shows a photograph of the purified yellow-colored GST-cCRY4 protein (708 μg/mL). (D) HPLC analysis of the GST-cCRY4 chromophore. The detailed protocol is described in Materials and Methods.

cCRY4 from a 10 L culture and 349 μg of nontagged cCRY4 from a 2.5 L culture (Figure 1A,B).

Chromophore FAD Bound to Recombinant cCRY4. The purified recombinant cCRY4 proteins were incubated overnight in the dark at 4 °C for complete oxidation of the chromophore FAD, because photointermediates might be produced during the purification process (see below). Then, the UV−visible absorption spectra were recorded, and a characteristic absorption pattern of oxidized flavin binding was identified (Figure 1C). The recombinant GST-cCRY4 sample was denatured by heat to extract the chromophore in a soluble fraction. HPLC analysis of the supernatant clearly indicated the consistent presence of FAD (Figure 1D). We estimated an amount of FAD in the heat-extracted fraction of GST-cCRY4 by comparing the peak value with that of the standard FAD sample. The amount of bound FAD was determined together with the protein concentration determined by an SDS−PAGE gel stained with Coomassie Brilliant Blue (CBB) using a series of diluted BSA standard samples as references, and the molar ratio of the FAD/GST-cCRY4 protein in the sample was estimated to be 1.14. Independently, we calculated the FAD/GST-cCRY4 ratio to be 1.25 assuming that the molar extinction coefficient of FAD in its binding pocket of cCRY4 is the same as that of the free FAD in solution (ε_{440} = 11300 M^{-1} cm^{-1}).[29] Although the sensitivity of the CBB staining might be different between GST-cCRY4 and BSA, these ratios (1.14−1.25) are consistent with the equimolar binding of FAD to the GST-cCRY4 protein in our preparation.

Light-Induced Structural Change Involving CCE of Recombinant cCRY4. Recombinant cCRY4 was immunoprecipitated under dark or blue light conditions to decipher whether there was a light-dependent interaction with C1 mAb (Figure 2). The relative amount of recombinant cCRY4 immunoprecipitated under light conditions (L in Figure 2B) was significantly smaller than that under dark conditions (D in Figure 2B), strongly suggesting that recombinant cCRY4 receives a photon without any factor(s) that changes its CCE structure. These results suggest that associating factors in the chicken retina are not required for cCRY4 photoreceptive properties.

Light-Dependent Change in Tryptic Digestion Sensitivity of cCRY4. To reveal whether the light-dependent dissociation of GST-cCRY4 from C1 mAb was associated with a CCE-specific structural change or an entire conformational change, we performed partial proteolysis of GST-cCRY4 (Figure 3). Upon partial tryptic digestion, the immunopositive band for full-length GST-cCRY4 (F1, Figure 3A, lane 1) disappeared, and F2−F6 fragments appeared (Figure 3A, lane 3). Because the C1 mAb epitope localized within CCE, the F2

DOI: 10.1021/bi501441u
Biochemistry 2015, 54, 1908−1917

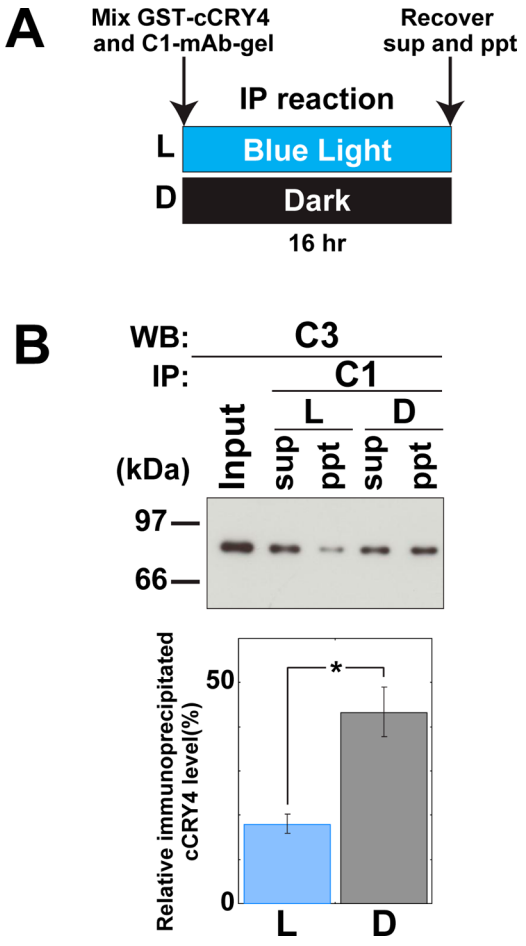

Figure 2. Light-dependent CCE structural change of GST-cCRY4. (A) Schematic drawing of the immunoprecipitation assay of GST-cCRY4. Purified GST-cCRY4 [in buffer containing 21.5 mM Tris-HCl (pH 7.5), 147.5 mM NaCl, 0.95 mM DTT, 9.5% (v/v) glycerol, 0.095% Tween 20, and Complete EDTA free protease inhibitor mixture (Roche Applied Sciences)] and C1-mAb-gel were mixed, and an immunoprecipitation reaction was performed at 4 °C for 16 h under light (L, 471 nm; 424 μW/cm^2)[28] or dark (D, covered with aluminum foil) conditions. (B) Immunoblot analysis of immunoprecipitants and supernatants. The immunoprecipitation reaction, recovering the supernatants, and washing of C1-mAb-gel were performed under the indicated light conditions. The relative immunoprecipitated level of GST-cCRY4 was calculated by dividing the signal intensity of ppt by that of sup plus ppt (n = 3). Error bars represent the standard deviation. *p < 0.05 (Student's t test). C1, C1 mAb that recognizes the carboxyl-terminal region of cCRY4 (Gln494–Lys507). C3, C3 mAb that recognizes the carboxyl-terminal region of cCRY4 (His512–Met525).

band (approximately 61 kDa) likely corresponds to cCRY4 generated by trypsin cleavage around the linker region between GST and cCRY4 (Figure 3B). Just below the bands for the F2 fragments, F3 fragments (approximately 58 kDa) were detected regardless of the lighting conditions. Signals for F4 (approximately 32 kDa), F5 (approximately 30 kDa), and F6 (approximately 26 kDa) bands were noticeably stronger when GST-CRY4 was digested by trypsin in the dark versus the light (Figure 3A).

Photoreduction of cCRY4 by Blue Light. Regardless of the presence of the GST tag, cCRY4 showed an absorption pattern characteristic of the CRY/PL family proteins with an oxidized FAD chromophore (Figure 1C, GST-cCRY4; Figure

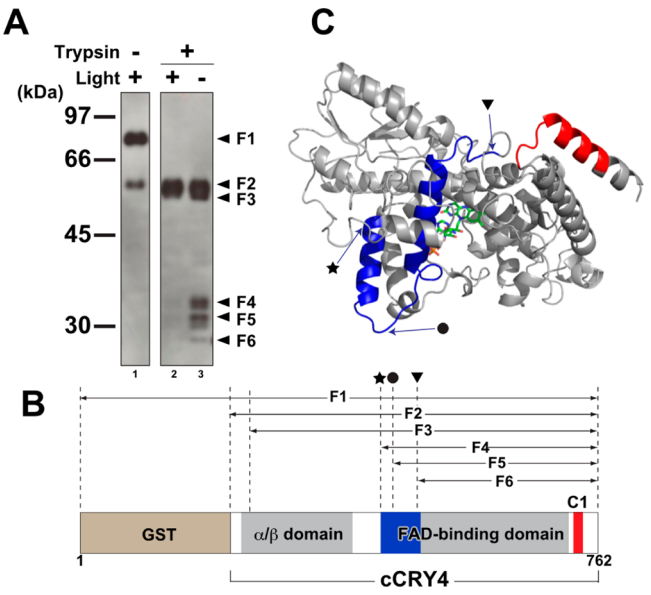

Figure 3. Partial proteolysis of GST-cCRY4 by trypsin under light or dark conditions. (A) Tryptic digestion of GST-cCRY4 under light [349 nm, black fluorescent lamp (SANKYO DENKI), 1 mW/cm^2] and dark (covered with aluminum foil) conditions. Tryptic digests are labeled F1–F6. (B) Estimated trypsin digestion sites in the GST-cCRY4 primary structure. The approximate molecular masses of fragments are 79, 61, 58, 32, 30, and 26 kDa for F1–F6, respectively. The calculated molecular mass of GST-cCRY4 is 88094 Da. C1, C1-mAb epitope. (C) Trypsin digestion sites in a predicted cCRY4 three-dimensional structure. In panels B and C, predicted light-dependent tryptic digestion sites (black stars, black circles, and black triangles) in the N-terminal part of the FAD-binding domain (blue-colored regions) and C1-mAb epitope (red-colored regions) are indicated. A simple sequence replacement model of cCRY4 (Phe9–Glu515) was constructed on the basis of *Arabidopsis thaliana* (6-4) PL (Protein Data Bank entry 3fy4B) with the aid of the MATRAS server.

4A,C, dark). Therefore, we chose to use nontagged cCRY4 for further spectroscopic analyses (Figures 4–6). Upon blue light irradiation (453 nm, 1 mW/cm^2) at 20 °C, absorption peaks at around 370 and 447 nm showed a decrease within 0.5 min, and the peak at around 500–650 nm (586 and 632 nm, respectively) showed an increase, most likely because of photic generation of a semiquinone radical intermediate having an FADH$^\bullet$ chromophore (FADH$^\bullet$ form) from the FADox form (Figure 4A,B). Further irradiation induced a decrease in the absorption bands at around 370, 447, and 500–650 nm (Figure 4A,B, curves 1 min–8 min). We believe the decrease in absorption in the longer wavelength regions was most likely due to a reduction of FADH$^\bullet$ to its fully reduced FADH$^-$ form because such a change was not observed when the semiquinone radical intermediate was incubated in the dark (see Figure 5C). To investigate the effect of temperature on photoreduction of the FAD chromophore, we compared the cCRY4 photocycle at 20 and 4 °C (Figure 4). When the formation of FADH$^\bullet$ and FADH$^-$ was monitored by a decrease in the level of the FADox form at 447 nm, the reaction is not dependent on temperature (Figure 4E). The formation of the FADH$^-$ also seems to lack temperature dependency, judging from the decrease in the level of FADH$^\bullet$ at 630 nm (Figure 4F).

Photoreduction by Red Light and Dark Oxidation of the FADH$^\bullet$ Form. In the case of *Chlamydomonas reinhardtii* aCRY,[30,31] red light irradiation of FADH$^\bullet$ also resulted in the formation of the FADH$^-$ form; therefore, we examined the

DOI: 10.1021/bi501441u
Biochemistry 2015, 54, 1908–1917

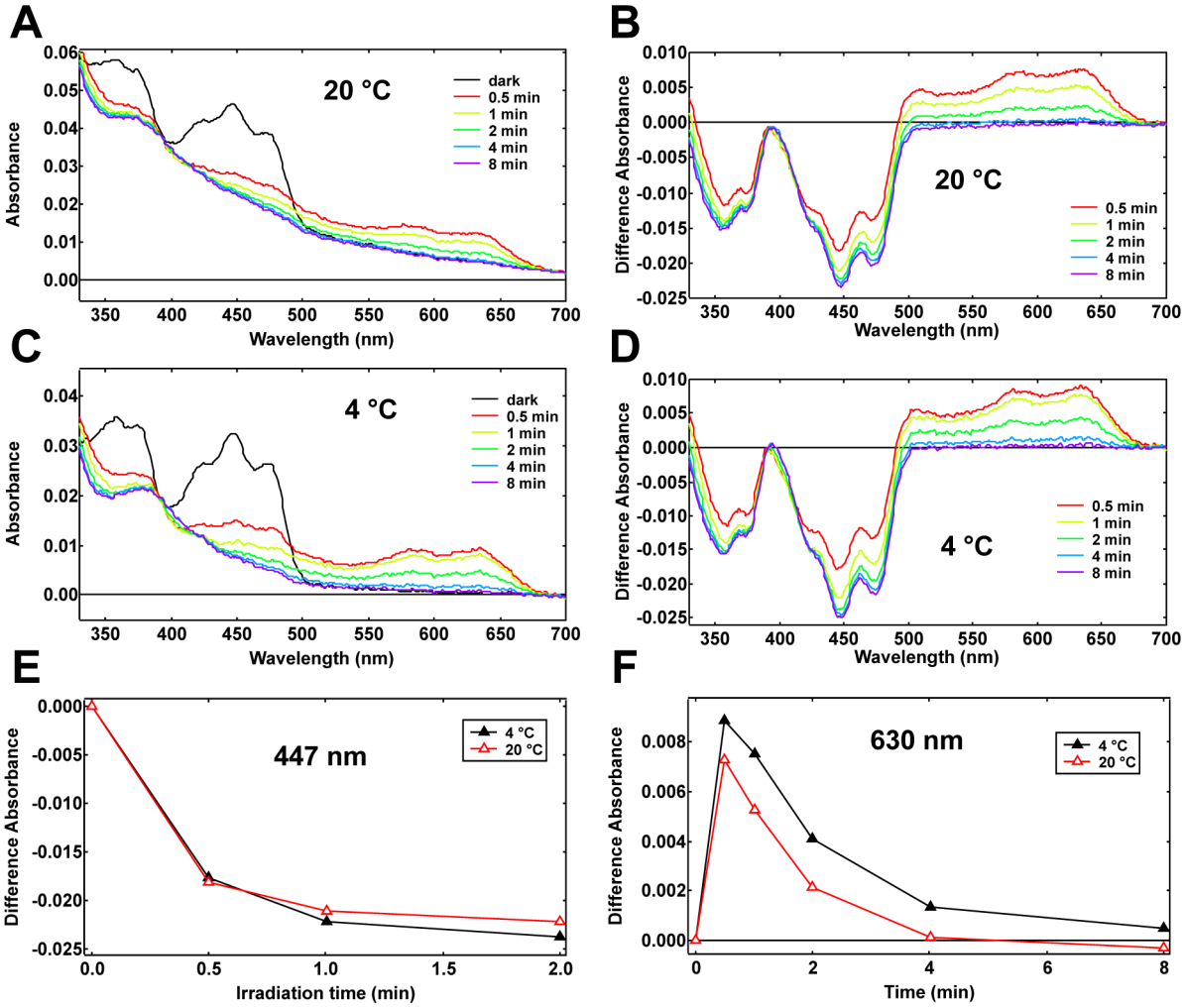

Figure 4. Blue light-induced spectral change of nontagged cCRY4. (A) Spectral changes of cCRY4 caused by blue light irradiation (total of 0.5−8 min, 453 nm, 1 mW/cm^2) at 20 °C. (B) Light minus dark differences in absorption spectra of cCRY4 shown in panel A. (C) Spectral changes of cCRY4 caused by blue light irradiation (total of 0.5−8 min, 453 nm, 1 mW/cm^2) at 4 °C. (D) Light minus dark differences in the absorption spectra of cCRY4 shown in panel C. (E) Effects of temperature on the formation of cCRY4 FADH$^\bullet$ monitored by the difference in absorbance at 447 nm. (F) Effects of temperature on the formation of cCRY4 FADH$^-$ monitored by the difference in absorbance at 630 nm.

long wavelength sensitivity of FADH$^\bullet$ in cCRY4 (Figure 5). There was decreased absorption at around 500−650 nm with red light irradiation of FADH$^\bullet$ (Figure 5A,B). In this case, absorption changes in the shorter wavelength region (300−500 nm) were minimal and quite different from those observed when FADH$^\bullet$ was oxidized to FADox under dark conditions (Figure 5C). When the difference absorption spectra of cCRY4 (Figure 5B) and those reported for *C. reinhardtii* aCRY are taken into consideration, we concluded that the FADH$^\bullet$ form in cCRY4 was reduced to FADH$^-$ with red light irradiation as was the case with *C. reinhardtii* aCRY.

Photoreduction of cCRY4 by White Light and Dark Oxidation of the FADH$^-$ Form. Blue light irradiation of the FADox form of cCRY4 caused the generation of FADH$^\bullet$ with absorption bands at around 500−650 nm, followed by chromophore photoreduction to FADH$^-$ with extended blue light (Figure 4A−D) or red light irradiation (Figure 5A,B). These results led us to investigate the photoreaction of cCRY4 under the more physiological condition, i.e., white light irradiation at the body temperature of the chicken (42 °C). Like blue light irradiation, white light irradiation likely photoreduced the FADox form to the FADH$^-$ form with transient formation of the FADH$^\bullet$ form in the short irradiation time (Figure 6A). Incubation of the FADH$^-$ form resulted in the complete oxidation to FADox under the dark conditions within 8 h (Figure 6B).

Light-Dependent Structural Change of cCRY4 Likely Occurs during Photoreduction of FADox to FADH$^\bullet$. As a first step in understanding the intramolecular photoreception mechanism of cCRY4, we examined whether the light-dependent structural change of cCRY4 occurred in FADH$^\bullet$ by comparing temporal profiles of the structural and spectroscopic changes (Figure 7). Chick retinal homogenates were incubated in the dark on a C1-mAb-immobilized gel to immunoprecipitate cCRY4, and then the gel was irradiated with blue light (471 nm, 100 μW/cm^2).[28] The amount of cCRY4 that dissociated from the C1 mAb-cCRY4 immunocomplex was measured using immunoblot analysis of the supernatants recovered at various time points. Retinal cCRY4 was released from the C1 mAb-gel within 0.75 min, which is the time point when the FADH$^\bullet$ form is produced, not the fully reduced form (Figure 7). The estimated time course of their dissociation [Figure 7B (●)] seemed to be similar to that for FADH$^\bullet$ accumulation measured by spectroscopy [Figure 7B (□)].

DOI: 10.1021/bi501441u
Biochemistry 2015, 54, 1908−1917

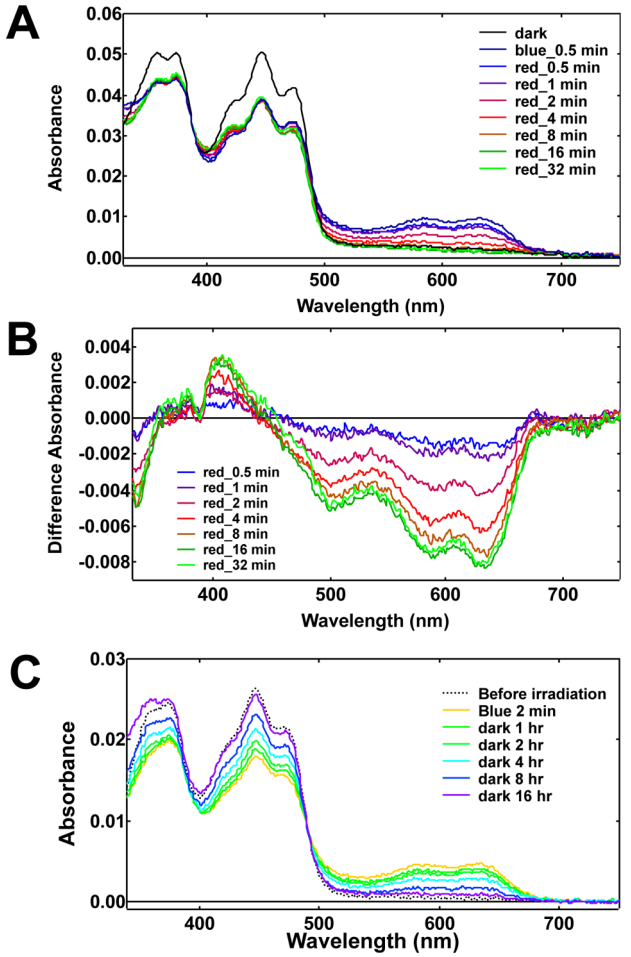

Figure 5. Photoreduction by red light and dark oxidation of the $FADH^{\bullet}$ form of nontagged cCRY4. (A) Absorbance changes of $FADH^{\bullet}$ in cCRY4 upon red light irradiation (628 nm, 0.7 mW/cm^2). $FADH^{\bullet}$ was generated by blue light irradiation for 0.5 min (448 nm, 1 mW/cm^2) of the FADox form, and then the sample was irradiated with red light (total of 0.5−32 min). The temperature was kept at 4 °C during measurement. (B) Differences in absorption spectra before and after red light irradiation (red minus blue). (C) Dark oxidation of the $FADH^{\bullet}$ form of cCRY4. $FADH^{\bullet}$ was generated by blue light irradiation (450 nm, 1 mW/cm^2) of the FADox form for 2 min (Blue 2 min). After the formation of $FADH^{\bullet}$, absorption spectra were recorded under dark conditions (1, 2, 4, 8, and 16 h). Time periods for dark incubation are given. The spectrum of the dark sample (before blue light irradiation) is shown with a dotted line. The temperature was kept at 20 °C during measurement.

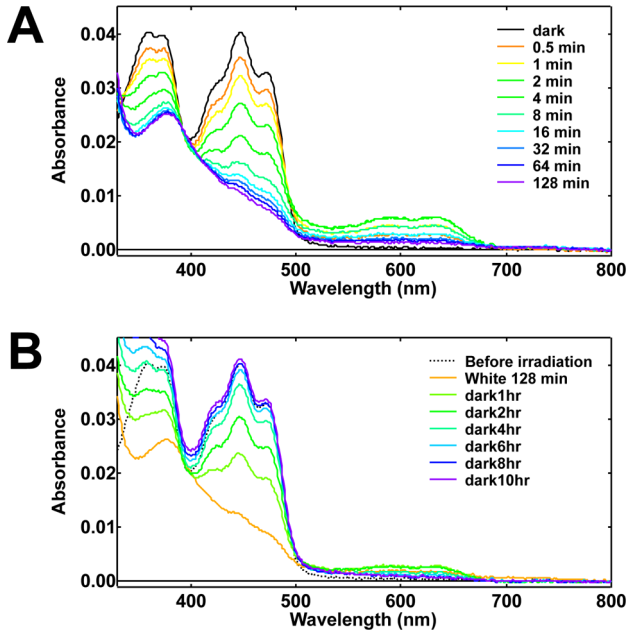

Figure 6. Photoreduction of FADox form of nontagged cCRY4 by white light and dark oxidation of the $FADH^-$ form at 42 °C. (A) Generation of $FADH^-$ from FADox with white light irradiation (1 mW/cm^2; total of 0.5−128 min) in nontagged cCRY4 at 42 °C. (B) Dark oxidation of the $FADH^-$ form. After white light irradiation for 128 min (A), absorption spectra were recorded under dark conditions at 42 °C (1, 2, 4, 6, 8, and 10 h, total incubation period). The spectrum of the dark sample (before white light irradiation) is shown with a dotted line.

These results imply that light-induced structural change in cCRY4 may occur during or just after reduction of the FADox chromophore. However, it is difficult to fully exclude a possibility of two-photon reaction (photoreduction of FADox to $FADH^-$) after irradiation for 0.75 min. This point could be examined by further comparative analysis of these temporal profiles at the beginning of the photoreaction, in which the photic release of retinal cCRY4 from C1 mAb would show quadratic behavior indicative of the two-photon reaction.

DISCUSSION

Overexpression and Purification of Chicken CRY4. In this study, we report a constitutive expression system for cCRY4 in budding yeast MaV203. In preliminary experiments, we tried to overexpress recombinant cCRY4 in *Escherichia coli* and insect cells, but we could not obtain a sufficient amount of cCRY4 protein for spectroscopic analysis. The baculovirus expression system is conventionally used for the expression of recombinant CRY proteins,[8,10,11,26] and there are a couple reports of systems using yeast cells in which the expression of exogenous proteins could be induced in *Schizosaccharomyces pombe*[32] and *Pichia pastoris*.[33] We believe our constitutive expression system may be more convenient than other systems because of the ease with which it can be scaled up for preparation of a large amount of CRY proteins.

Light-Induced Structural Change of cCRY4. We demonstrated in a previous study that the interaction between retinal cCRY4 and C1 mAb changes in a light-dependent manner.[24] While this may mean that light initiates a dynamic structural change that includes CCE, there is still the possibility that a retinal factor locally modifies the C1 epitope in CCE and alters immunoreactivity to C1 mAb with light irradiation. Another possibility is that other retinal phototransduction proteins such as the opsins or rhodopsin kinase assist with photic changes. This study was undertaken using recombinant cCRY4 protein without retinal factor(s). On the basis of our results, we concluded that cCRY4 itself retained photosensitivity to change its structure dynamically during photic changes with immunoprecipitation (Figure 2) and protease resistance (Figure 3).

The light-dependent change in trypsin resistance (Figure 3) led us to infer a possible site for the structural changes. Because the C1 mAb epitope is located in the proximity of the C-terminus, we were able to map putative trypsin cleavage sites that could produce F4−F6 fragments. Those sites with trypsin resistance only in light were mapped at a region close to the

DOI: 10.1021/bi501441u
Biochemistry 2015, 54, 1908−1917

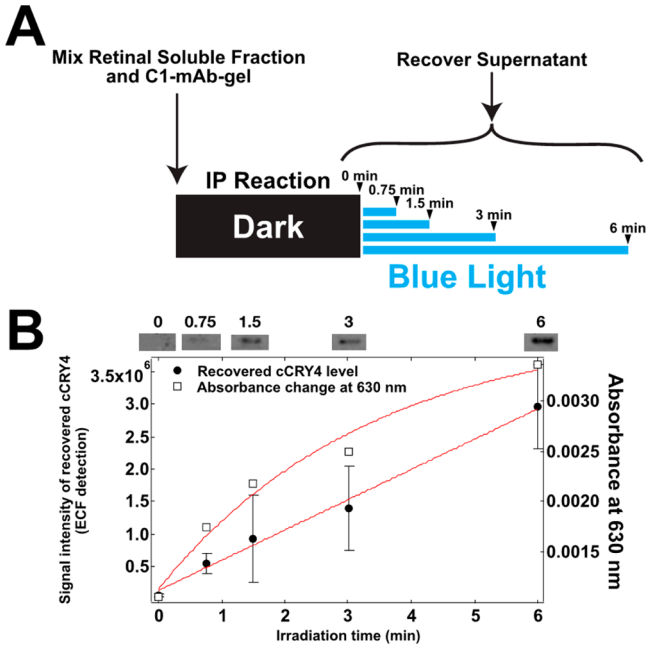

Figure 7. *In vitro* comparative analysis of time courses for the structural and spectral changes of recombinant cCRY4. (A) Schematic drawing of the assay. (B) Time courses of the dissociation of retinal cCRY4 from C1 mAb and generation of FADH$^{\bullet}$ from FADox upon blue light irradiation of recombinant nontagged cCRY4 (86 μg/mL) at 22 °C. Immunoprecipitation of chick retinal cCRY4 using C1 mAb was performed according to the experimental procedure described in ref 24. In brief, chick retinas were homogenized in lysis buffer containing 1 mM DTT (detailed composition of the buffer is described in ref 24), and the immunocomplex containing cCRY4 was precipitated from the retinal extract with C1 mAb in the dark and irradiated with blue light (471 nm, 100 μW/cm^2)[28] for 0.75, 1.5, 3.0, and 6.0 min. Then the amounts of cCRY4 recovered in supernatants were estimated by immunoblot analysis using C1 mAb. Representative examples of cCRY4 immunoblot signals at each time point are shown above the plot. Black circles show the signal intensity of cCRY4 recovered in the supernatant. Quantification of signal intensity was performed using ImageQuantTL (GE Healthcare). Error bars represent the standard deviation of the mean. White squares show the cCRY4 absorbance changes at 630 nm during blue light (461 nm, 100 μW/cm^2) irradiation under the same buffer conditions except without protease inhibitors.

FAD-binding domain within the PHR [see Figure 3C, blue region; predicted cCRY4 3D structure with the aid of MATRAS using structural data for *Arabidopsis thaliana* (6-4) photolyase (Protein Data Bank entry 3fy4B) as the template]. This region may be highly accessible to trypsin in the dark and less accessible in the light. Together with the light-dependent change in the accessibility of C1 mAb to its epitope in the CCE region (red-colored region in Figure 3C), one plausible explanation is that the CCE region may move to bind to the FAD-binding domain in the light, which makes it more difficult for trypsin and C1-mAb to access the FAD-binding domain and C1-mAb epitope, respectively.

Previous studies of *A. thaliana* CRY1 (AtCRY1) and the *Drosophila melanogaster* CRY (dCRY) reported that the CCE and PHR of these CRYs bind together in the dark and dissociate with light irradiation.[12,14,34−36] The light-dependent dissociation allows binding with COP1 or JETLAG, each a downstream signaling molecule for AtCRY1 or dCRY, respectively,[14,37] and triggers the phototransduction cascade. Considering that cCRY4 is opposite in nature in that the CCE region seems to bind with PHR with a light signal, a possible downstream effector for cCRY4 may bind to cCRY4 in the dark. Future investigation of molecules that interact with cCRY4 would help to better understand the physiological functions of cCRY4.

Photocycle of cCRY4. By short durations of cCRY4 irradiation with blue light (Figures 4 and 5), we detected reduction of the FADox chromophore to FADH$^{\bullet}$, which was not observed in the previous study by Oztürk et al.[26] Extended durations of irradiation reduced FADH$^{\bullet}$ to the FADH^{-} form (Figures 4 and 5). We detected for the first time that the FADH^{-} form returned to FADox in the dark via FADH$^{\bullet}$ formation (Figure 6), and we could depict the putative photocycle of cCRY4 (Figure 8A). Although the dark oxidation of FADH^{-} to the FADH$^{\bullet}$ form was observed in the previous study,[26] their observations are not fully congruent with the photocycle shown in Figure 8A, probably because there are many differences in experimental conditions such as the different irradiation wavelengths (UV-A or blue light), the light intensity, the expression system used, the presence of the FLAG tag, and perhaps concentration of dissolved oxygen.

The reduction from FADox to FADH$^{\bullet}$ is likely composed of two steps; (i) electron transfer to FADox to generate FAD$^{\bullet-}$ anion radical and (ii) its protonation to generate the neutral FADH$^{\bullet}$ form.[38] We did not observe temperature dependency in this reduction process (Figure 4), implying that both of these steps might be composed of temperature-independent mechanisms under the experimental conditions presented here.

We further estimated the absolute absorbance spectra of FADox, FADH$^{\bullet}$, and FADH^{-} forms (Figure 8B) using the difference absorption spectra obtained from our present measurements (Figures 5 and 6). Then, by using the photon fluence rate, the absorbance of the sample, and the rate of photoreaction of FADox to FADH$^{\bullet}$ (Figure 5, blue light irradiation), we could roughly estimate the quantum yield for the photoreduction (Φ_1) to be ≈3%. Similarly, the quantum yield for the photoreduction of FADH$^{\bullet}$ to FADH^{-} (Φ_2) (Figure 5, red light irradiation) was estimated to be ≈2%. These values are lower than the quantum yields for the photoreduction of the other cryptochromes such as *Chlamydomonas* aCRY ($\Phi_1 \approx 7\%$[31]), but these values may be enough to receive an external light or magnetic signals accounting for the wide and relatively strong expression of cCRY4 in the retina.

The speculated photocycle of cCRY4 (Figure 8A) is similar to that of AtCRY1,[8] but in the case of AtCRY1, FADH$^{\bullet}$ was not detected spectroscopically when FADH^{-} was incubated in the dark for reoxidation to FADox.[39] This may be due to the rapid oxidation of FADH$^{\bullet}$ to FADox in the two-electron reoxidation process of AtCRY1.

In this study, both the FADH$^{\bullet}$ and FADH^{-} forms of cCRY4 were oxidized *in vitro* under dark conditions (Figures 5C and 6B). A recent study of chicken CRY1a (cCRY1a),[40] another CRY identified in the chicken retina, implied that cCRY1a may absorb not only blue light but also that of longer wavelengths (e.g., green and yellow) utilizing the FADH$^{\bullet}$ state and changing its CCE conformation in the FADH^{-} state. Nießner et al.[40] analyzed cCRY1a activation using the chicken retina *in vivo*; therefore, future investigation extending our novel yeast expression system to other CRY proteins both *in vivo* and *in vitro* may be beneficial to further analyses.

DOI: 10.1021/bi501441u
Biochemistry 2015, 54, 1908−1917

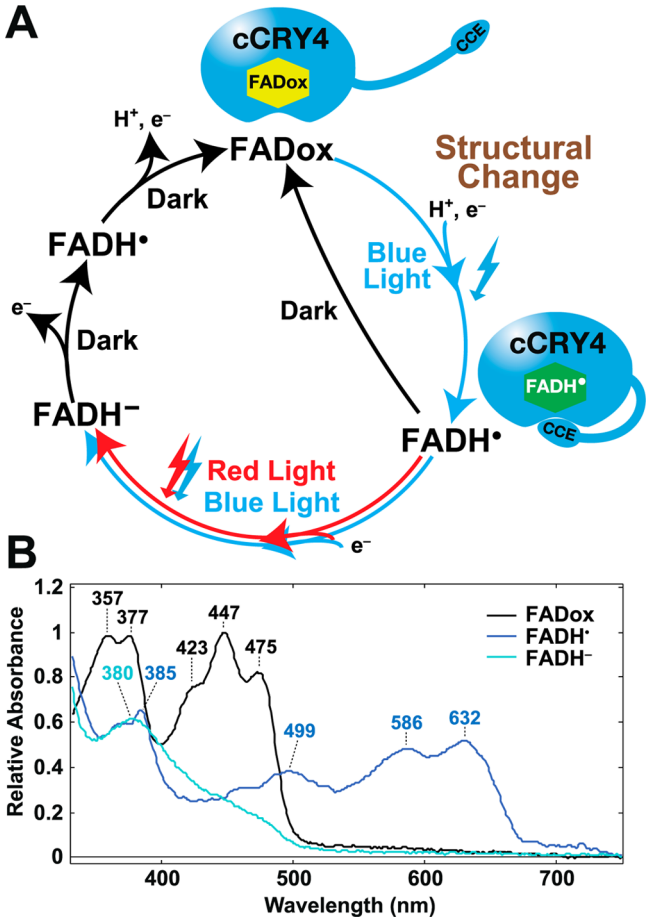

Figure 8. Model for the cCRY4 photocycle and calculated absolute absorbance spectra of photointermediates. (A) Short duration (0.5 min) irradiation with blue light (453 nm, 1 mW/cm^2) reduced the FADox chromophore to the FADH$^•$ form. Extended blue light or red light irradiation further reduced FADH$^•$ to FADH$^-$. FADH$^•$ is likely oxidized to FADox directly in dark, while FADH$^-$ is likely oxidized to FADox via FADH$^•$ during dark incubation. (B) Absolute absorbance spectra of cCRY4 photointermediates estimated by calculation. The dark-adapted samples ("dark" in Figure 5A and "dark" in Figure 6A) are considered to be mainly composed of FADox with a small amount of residual FADH$^•$. The sample, after a long irradiation with white light (128 min, 1 mW/cm^2), is presumed to be composed of only FADH$^-$ forms. Spectral changes induced by the initial 0.5 min blue light and the following 8 min red light irradiations in Figure 5A are assumed to correspond to conversions from FADox to FADH$^•$ and FADH$^•$ to FADH$^-$, respectively. The absorbance spectra were estimated using the spectra of "dark", "blue_0.5 min", and "red_8 min" in Figure 5A and "dark" and "white_128 min" in Figure 6A as follows. (i) All spectra were normalized by their optical density and presumed to have absorbances at the peak of the dark-adapted spectrum such that the FADox form (447 nm) was 1.0. Absorbances at putative isosbestic points between the FADH$^•$ and FADH$^-$ forms (446 nm, red_8 min in Figure 5B) or the FADox and FADH$^-$ forms were used (392 nm, Figure 6A). (ii) When the putative photobleaching rates of FADox were changed from 20 to 50%, putative absolute absorption spectra for FADH$^•$ were calculated and the photobleaching rate was determined to be 31%, placing the isosbestic point between FADH$^•$ and FADH$^-$ at 446 nm. (iii) The determined absolute absorption spectrum of FADH$^•$ was diminished from "dark" or "white_128 min" in the spectrum in Figure 6A with changing putative contents of the contaminating FADH$^•$ form. We inferred the FADH$^•$ content in the FADox and FADH$^-$ forms to be 3%, assuming that FADox had no absorbance in the longer wavelength region (>520 nm).

Biological Functions of CRY4. Avian CRYs are thought to work as light-driven magnetoreceptors[25] based on their localization in the retina[24,41,42] and the photosensitivity of the purified protein.[43,44] On the other hand, in the Western clawed frog, CRY4 is highly expressed in the ovary and testis rather than the retina[22] and hence more likely to be implicated in unknown photic function(s) in the gonadal tisses instead of magnetoreception. Considering that CRY involves multiple functions such as nonvisual photoreception,[5,45] magnetoreception,[7] and vision,[46] CRY4 may play multiple roles in different cells and/or organs.

AUTHOR INFORMATION

Corresponding Author

*Department of Electrical Engineering and Bioscience, Graduate School of Advanced Science and Engineering, Waseda University, Wakamatsu-cho 2-2, Shinjuku-ku, Tokyo 162-8480, Japan. Telephone and fax: +81-3-5369-7316. E-mail: okano@waseda.jp.

Funding

This work was partially supported by the Grants-in-Aid from the Ministry of Education, Culture, Sports, Science and Technology (MEXT), the Research Foundation for Opto-Science and Technology, and the Japan Society for the Promotion of Science (JSPS, 23248033, 24657109, and 26650024) of Japan awarded to T.O.

Notes

The authors declare no competing financial interest.

ABBREVIATIONS

CRY, cryptochrome; PL, photolyase; PHR, photolyase homology region; cCRY, chicken CRY; AtCRY, *A. thaliana* CRY; dCRY, *D. melanogaster* CRY; CCE, cryptochrome carboxyl-terminal extension region; DBD, DNA-binding domain; AD, activation domain; DTT, dithiothreitol; FADox, fully oxidized form of FAD; FADH$^•$, neutral semiquinone radical form of FAD; FADH$^-$, fully reduced form of FAD.

REFERENCES

(1) Cashmore, A. R. (2003) Cryptochromes: Enabling plants and animals to determine circadian time. *Cell 114*, 537−543.

(2) Brettel, K., and Byrdin, M. (2010) Reaction mechanisms of DNA photolyase. *Curr. Opin. Struct. Biol. 20*, 693−701.

(3) Ahmad, M., and Cashmore, A. R. (1993) *HY4* gene of *A. thaliana* encodes a protein with characteristics of a blue-light photoreceptor. *Nature 366*, 162−166.

(4) Guo, H., Yang, H., Mockler, T. C., and Lin, C. (1998) Regulation of flowering time by *Arabidopsis* photoreceptors. *Science 279*, 1360−1363.

(5) Emery, P., So, W. V., Kaneko, M., Hall, J. C., and Rosbash, M. (1998) CRY, a Drosophila clock and light-regulated cryptochrome, is a major contributor to circadian rhythm resetting and photosensitivity. *Cell 95*, 669−679.

(6) Hirayama, J., Miyamura, N., Uchida, Y., Asaoka, Y., Honda, R., Sawanobori, K., Todo, T., Yamamoto, T., Sassone-Corsi, P., and Nishina, H. (2009) Common light signaling pathways controlling DNA repair and circadian clock entrainment in zebrafish. *Cell Cycle 8*, 2794−2801.

(7) Gegear, R. J., Casselman, A., Waddell, S., and Reppert, S. M. (2008) Cryptochrome mediates light-dependent magnetosensitivity in *Drosophila*. *Nature 454*, 1014−1018.

(8) Lin, C., Robertson, D. E., Ahmad, M., Raibekas, A. A., Jorns, M. S., Dutton, P. L., and Cashmore, A. R. (1995) Association of flavin

DOI: 10.1021/bi501441u
Biochemistry 2015, 54, 1908−1917

adenine dinucleotide with the *Arabidopsis* blue light receptor CRY1. *Science 269*, 968−970.
(9) Giovani, B., Byrdin, M., Ahmad, M., and Brettel, K. (2003) Light-induced electron transfer in a cryptochrome blue-light photoreceptor. *Nat. Struct. Biol. 10*, 489−490.
(10) Banerjee, R., Schleicher, E., Meier, S., Viana, R. M., Pokorny, R., Ahmad, M., Bittl, R., and Batschauer, A. (2007) The signaling state of *Arabidopsis* cryptochrome 2 contains flavin semiquinone. *J. Biol. Chem. 282*, 14916−14922.
(11) Berndt, A., Kottke, T., Breitkreuz, H., Dvorsky, R., Hennig, S., Alexander, M., and Wolf, E. (2007) A novel photoreaction mechanism for the circadian blue light photoreceptor *Drosophila* cryptochrome. *J. Biol. Chem. 282*, 13011−13021.
(12) Kondoh, M., Shiraishi, C., Muller, P., Ahmad, M., Hitomi, K., Getzoff, E. D., and Terazima, M. (2011) Light-induced conformational changes in full-length *Arabidopsis* thaliana cryptochrome. *J. Mol. Biol. 413*, 128−137.
(13) Li, X., Wang, Q., Yu, X., Liu, H., Yang, H., Zhao, C., Liu, X., Tan, C., Klejnot, J., Zhong, D., and Lin, C. (2011) *Arabidopsis* cryptochrome 2 (CRY2) functions by the photoactivation mechanism distinct from the tryptophan (trp) triad-dependent photoreduction. *Proc. Natl. Acad. Sci. U.S.A. 108*, 20844−20849.
(14) Ozturk, N., Selby, C. P., Annayev, Y., Zhong, D., and Sancar, A. (2011) Reaction mechanism of *Drosophila* cryptochrome. *Proc. Natl. Acad. Sci. U.S.A. 108*, 516−521.
(15) Vaidya, A. T., Top, D., Manahan, C. C., Tokuda, J. M., Zhang, S., Pollack, L., Young, M. W., and Crane, B. R. (2013) Flavin reduction activates *Drosophila* cryptochrome. *Proc. Natl. Acad. Sci. U.S.A. 110*, 20455−20460.
(16) Ozturk, N., Selby, C. P., Zhong, D., and Sancar, A. (2014) Mechanism of photosignaling by *Drosophila* cryptochrome: Role of the redox status of the flavin chromophore. *J. Biol. Chem. 289*, 4634−4642.
(17) Muller, P., Bouly, J. P., Hitomi, K., Balland, V., Getzoff, E. D., Ritz, T., and Brettel, K. (2014) ATP binding turns plant cryptochrome into an efficient natural photoswitch. *Sci. Rep. 4*, 5175.
(18) Kume, K., Zylka, M. J., Sriram, S., Shearman, L. P., Weaver, D. R., Jin, X., Maywood, E. S., Hastings, M. H., and Reppert, S. M. (1999) mCRY1 and mCRY2 are essential components of the negative limb of the circadian clock feedback loop. *Cell 98*, 193−205.
(19) Yamamoto, K., Okano, T., and Fukada, Y. (2001) Chicken pineal Cry genes: Light-dependent up-regulation of cCry1 and cCry2 transcripts. *Neurosci. Lett. 313*, 13−16.
(20) Kobayashi, Y., Ishikawa, T., Hirayama, J., Daiyasu, H., Kanai, S., Toh, H., Fukuda, I., Tsujimura, T., Terada, N., Kamei, Y., Yuba, S., Iwai, S., and Todo, T. (2000) Molecular analysis of zebrafish photolyase/cryptochrome family: Two types of cryptochromes present in zebrafish. *Genes Cells 5*, 725−738.
(21) Kubo, Y., Akiyama, M., Fukada, Y., and Okano, T. (2006) Molecular cloning, mRNA expression, and immunocytochemical localization of a putative blue-light photoreceptor CRY4 in the chicken pineal gland. *J. Neurochem. 97*, 1155−1165.
(22) Takeuchi, T., Kubo, Y., Okano, K., and Okano, T. (2014) Identification and characterization of cryptochrome4 in the ovary of western clawed frog *Xenopus tropicalis*. *Zool. Sci. 31*, 152−159.
(23) Ozturk, N., Song, S. H., Ozgur, S., Selby, C. P., Morrison, L., Partch, C., Zhong, D., and Sancar, A. (2007) Structure and function of animal cryptochromes. *Cold Spring Harbor Symp. Quant. Biol. 72*, 119−131.
(24) Watari, R., Yamaguchi, C., Zemba, W., Kubo, Y., Okano, K., and Okano, T. (2012) Light-dependent structural change of chicken retinal Cryptochrome4. *J. Biol. Chem. 287*, 42634−42641.
(25) Ritz, T., Adem, S., and Schulten, K. (2000) A model for photoreceptor-based magnetoreception in birds. *Biophys. J. 78*, 707−718.
(26) Ozturk, N., Selby, C. P., Song, S. H., Ye, R., Tan, C., Kao, Y. T., Zhong, D., and Sancar, A. (2009) Comparative photochemistry of animal type 1 and type 4 cryptochromes. *Biochemistry 48*, 8585−8593.
(27) Fields, S., and Song, O. (1989) A novel genetic system to detect protein-protein interactions. *Nature 340*, 245−246.
(28) Akiyama, M., Okano, K., Fukada, Y., and Okano, T. (2009) Macrophage inhibitory cytokine MIC-1 is upregulated by short-wavelength light in cultured normal human dermal fibroblasts. *FEBS Lett. 583*, 933−937.
(29) Damiani, M. J., Nostedt, J. J., and O'Neill, M. A. (2011) Impact of the N5-proximal Asn on the thermodynamic and kinetic stability of the semiquinone radical in photolyase. *J. Biol. Chem. 286*, 4382−4391.
(30) Beel, B., Prager, K., Spexard, M., Sasso, S., Weiss, D., Muller, N., Heinnickel, M., Dewez, D., Ikoma, D., Grossman, A. R., Kottke, T., and Mittag, M. (2012) A flavin binding cryptochrome photoreceptor responds to both blue and red light in *Chlamydomonas reinhardtii*. *Plant Cell 24*, 2992−3008.
(31) Spexard, M., Thoing, C., Beel, B., Mittag, M., and Kottke, T. (2014) Response of the sensory animal-like cryptochrome aCRY to blue and red light as revealed by infrared difference spectroscopy. *Biochemistry 53*, 1041−1050.
(32) Sang, Y., Li, Q. H., Rubio, V., Zhang, Y. C., Mao, J., Deng, X. W., and Yang, H. Q. (2005) N-terminal domain-mediated homodimerization is required for photoreceptor activity of *Arabidopsis* CRYPTOCHROME 1. *Plant Cell 17*, 1569−1584.
(33) Vieira, J., Jones, A. R., Danon, A., Sakuma, M., Hoang, N., Robles, D., Tait, S., Heyes, D. J., Picot, M., Yoshii, T., Helfrich-Forster, C., Soubigou, G., Coppee, J. Y., Klarsfeld, A., Rouyer, F., Scrutton, N. S., and Ahmad, M. (2012) Human cryptochrome-1 confers light independent biological activity in transgenic *Drosophila* correlated with flavin radical stability. *PLoS One 7*, e31867.
(34) Partch, C. L., Clarkson, M. W., Ozgur, S., Lee, A. L., and Sancar, A. (2005) Role of structural plasticity in signal transduction by the cryptochrome blue-light photoreceptor. *Biochemistry 44*, 3795−3805.
(35) Levy, C., Zoltowski, B. D., Jones, A. R., Vaidya, A. T., Top, D., Widom, J., Young, M. W., Scrutton, N. S., Crane, B. R., and Leys, D. (2013) Updated structure of *Drosophila* cryptochrome. *Nature 495*, E3−E4.
(36) Muller, P., and Bouly, J. P. (2015) Searching for the mechanism of signalling by plant photoreceptor cryptochrome. *FEBS Lett. 589*, 189−192.
(37) Liu, H., Liu, B., Zhao, C., Pepper, M., and Lin, C. (2011) The action mechanisms of plant cryptochromes. *Trends Plant Sci. 16*, 684−691.
(38) Liu, B., Liu, H., Zhong, D., and Lin, C. (2010) Searching for a photocycle of the cryptochrome photoreceptors. *Curr. Opin. Plant Biol. 13*, 578−586.
(39) Muller, P., and Ahmad, M. (2011) Light-activated cryptochrome reacts with molecular oxygen to form a flavin-superoxide radical pair consistent with magnetoreception. *J. Biol. Chem. 286*, 21033−21040.
(40) Niessner, C., Denzau, S., Stapput, K., Ahmad, M., Peichl, L., Wiltschko, W., and Wiltschko, R. (2013) Magnetoreception: Activated cryptochrome 1a concurs with magnetic orientation in birds. *J. R. Soc., Interface 10*, 20130638.
(41) Mouritsen, H., Janssen-Bienhold, U., Liedvogel, M., Feenders, G., Stalleicken, J., Dirks, P., and Weiler, R. (2004) Cryptochromes and neuronal-activity markers colocalize in the retina of migratory birds during magnetic orientation. *Proc. Natl. Acad. Sci. U.S.A. 101*, 14294−14299.
(42) Niessner, C., Denzau, S., Gross, J. C., Peichl, L., Bischof, H. J., Fleissner, G., Wiltschko, W., and Wiltschko, R. (2011) Avian ultraviolet/violet cones identified as probable magnetoreceptors. *PLoS One 6*, e20091.
(43) Liedvogel, M., Maeda, K., Henbest, K., Schleicher, E., Simon, T., Timmel, C. R., Hore, P. J., and Mouritsen, H. (2007) Chemical magnetoreception: Bird cryptochrome 1a is excited by blue light and forms long-lived radical-pairs. *PLoS One 2*, e1106.
(44) Du, X. L., Wang, J., Pan, W. S., Liu, Q. J., Wang, X. J., and Wu, W. J. (2014) Observation of magnetic field effects on transient fluorescence spectra of cryptochrome 1 from homing pigeons. *Photochem. Photobiol. 90*, 989−996.
(45) Tu, D. C., Batten, M. L., Palczewski, K., and Van Gelder, R. N. (2004) Nonvisual photoreception in the chick iris. *Science 306*, 129−131.

DOI: 10.1021/bi501441u
Biochemistry 2015, 54, 1908−1917

(46) Mazzotta, G., Rossi, A., Leonardi, E., Mason, M., Bertolucci, C., Caccin, L., Spolaore, B., Martin, A. J., Schlichting, M., Grebler, R., Helfrich-Forster, C., Mammi, S., Costa, R., and Tosatto, S. C. (2013) Fly cryptochrome and the visual system. *Proc. Natl. Acad. Sci. U.S.A. 110*, 6163−6168.

DOI: 10.1021/bi501441u
Biochemistry 2015, 54, 1908−1917